

1 Article

2 Mechanisms of obtaining secondary structures on 3 friction surface of experimental aluminum alloys for 4 monometallic journal bearings

5 Pavel Podrabinnik ^{1,*}, Iosif Gershman ^{1,2}, Alexander Mironov ^{1,2} and Ekaterina Kuznetsova ¹

6 ¹ Moscow State University of Technology «STANKIN», Vadkovsky lane 3a, 127055 Moscow, Russia;
7 p.podrabinnik@stankin.ru (P.P.); isgershman@gmail.com (I.G.); lecast@stankin.ru (A.M.)
8 evkuznetsova11@gmail.com (E.K.)

9 ² Railway Research Institute JSC "VNIIZHT", 3rd Mytischinskaya Street 10, 107996 Moscow, Russia.

10 * Correspondence: p.podrabinnik@stankin.ru; Tel.: +7-499-972-9494

11

12 **Abstract:** Within the task of replacing bronze journal bearings with aluminum the processes taking
13 part on friction surface of high-alloyed aluminum alloys working with steel are investigated. The
14 surface and subsurface layer of experimental aluminum bearings were studied before and after
15 tribological tests by scanning electron microscopy including energy-dispersive analysis. Both
16 structural and composition changes in surface layer are shown. It has been revealed that secondary
17 structures are formed on the surface during friction process and include all the chemical elements
18 of the tribosystem which is a consequence of its self-organization. The interaction behavior of some
19 chemical elements of tribological system is discussed.

20 **Keywords:** aluminum alloys; bronze; journal bearings; tribological alloys; friction; friction surface;
21 secondary structures; self-organization.

22

23 1. Introduction

24 Today the most of cast monometallic journal bearings are made of antifriction bronzes of
25 various grades. On railway transport the most common is bronze BrO4Z4S17 (closest analogue
26 C83800 Brass according to ASTM B271, B505, B584) due to its mechanical and tribotechnical
27 properties, which consumes more than 1.5 thousand tons of bronze per year. The task of increasing
28 the economic efficiency of the production and operation of bearings always remains relevant, given
29 the relatively high cost of copper, the main component of bronze. In this connection, the problem of
30 replacing monometallic bronze journal bearings with bearings based on aluminum alloys is solving
31 [1-7]. The transition from bronze to aluminum alloys is economically advantageous - aluminum is 3
32 times lighter than copper, and one kilogram of aluminum alloy is 2.5 to 2.7 times cheaper than
33 bronze. Aluminum alloys are more fusible and, consequently, their smelting is less
34 energy-consuming and takes less time, which makes it 15-20% cheaper. At the same time mechanical
35 processing of bronze is 10 to 12% more expensive comparing to aluminum alloys.

36 The first works on the study of aluminum journal bearings have shown that multicomponent
37 aluminum alloys can outperform the bronze in tribotechnical characteristics and have the potential
38 to achieve the required mechanical properties [2, 8]. The advantages of such aluminum alloys over
39 bronze BrO4C4S17 in tribological properties are associated with a greater ability to self-organization
40 of complex alloyed aluminum alloy and the formation on its surface a layer of protective secondary
41 structures different from the initial state of the material [4, 6, 9]. For a more detailed understanding
42 of the friction process, it is necessary to establish the principles of elements interaction in the system
43 for the secondary structures formation on the aluminum alloy surface. There is an approach in
44 which the selection of optimal sliding bearings is based on the principle of their least wear by
45 introducing solid inclusions: carbides, oxides and nitrides [10]. The disadvantage of this approach is

46 the complete disregard of the wear intensification of the counterbody, which is the more expensive
47 steel shaft.

48 2. Materials and Methods

49 Eight experimental cast aluminum alloys were used in the study. The composition of each alloy
50 included tin, lead, copper, silicon, magnesium and zinc as alloying components. The strength tests
51 were carried out in accordance with GOST 1497-84 on cylindrical samples with an estimated length
52 of 30 mm and a diameter of 6 mm on an electromechanical test machine "Instron" (USA).
53 Tribotechnical tests were carried out using a friction machine "SMC-2" with a loading device up to
54 3000 N. The composition control of each alloy after casting was performed by emission spectrometer
55 Spectrolab-S (USA). The study of the initial state, friction surfaces and secondary structures of
56 experimental alloys was performed on a Scanning Electron Microscope (SEM) "Tescan Vega 3"
57 (Czech Republic) equipped with an Oxford Instruments (UK) energy-dispersive analysis (EDX)
58 module. Before being placed in a microscope, the friction surfaces of the samples were rubbed with
59 alcohol and dried, the cross-sections were further polished to remove the oxide film. All samples
60 were examined at three magnifications: 100, 500 and 5000 times using secondary and back-scattered
61 electron detectors. For each of the specimen studied, EDX was used to compile maps of chemical
62 elements distribution, the distribution of elements along the line, and also the elemental composition
63 in local areas of 1 μm^2 .

64 3. Results and discussion

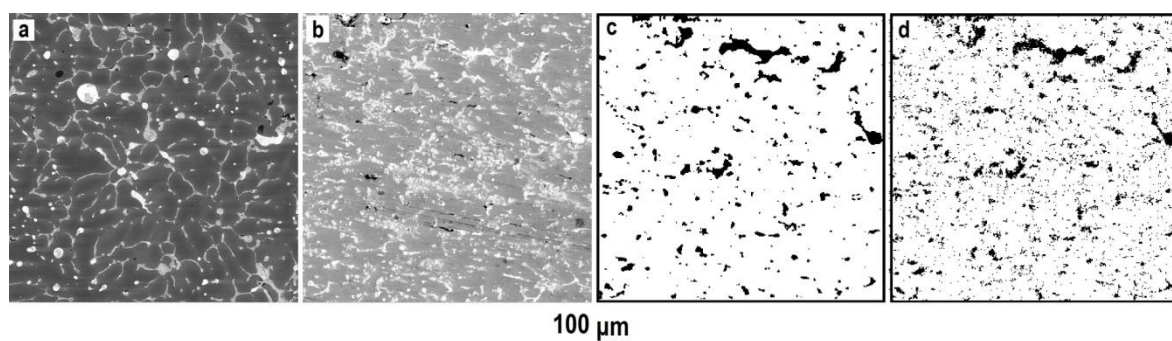
65 Of the 8 experimental alloys, the AO-5.8 alloy was chosen because of the lowest wear rates of
66 both the alloy and the steel counterbody: 0.4 and 0.6 mg, respectively, during the test period. The
67 composition of the alloy AO-5.8 is shown in Table 1. The presence of oxygen and carbon on the
68 surface of the alloys of the initial samples, detected by EDX, is caused by the presence of residues of
69 polishing components like suspensions and the onset of the oxidation process.

70 **Table 1.** AO-5.8 Elements composition.

Object	Elements composition, % mass.												
	Al	Sn	Pb	Cu	Zn	Si	Mg	Ti	C	O	Fe	S	Ca
As cast	82.1	5.8	2.7	4.1	2.3	1.5	1.5	-	-	-	-	-	-
Initial surface	77.7	3.7	2.1	2.9	2.2	1.8	0.3	0.1	5.1	3.9	0.1	-	-
Friction surface	40.5	3.9	4.7	2.0	1.5	0.4	0.6	-	31.4	14.5	0.3	-	0.1
Local spectra analysis													
Al matrix	72.1	-	-	0.8	1.3	0.2	0.2	-	14.3	10.8	-	-	0.2
Pb inclusion	0.5	1.7	71.8	1.3	1.0	0.2	0.2	-	20.1	3.1	-	0.2	-
Sn inclusion	1.5	23.5	16.8	-	1.0	0.1	5.8	-	20.2	30.5	-	-	0.5

71 The friction surface of the alloy after 40 hours of run-in significantly differs from the initial one
72 both in structure (Figure 1a, b) and in the qualitative elemental composition (Table 1). The result of
73 these changes was the formation of secondary structures on the friction surface of the alloy. The
74 formation of such secondary structures is a complex process of self-organization of the friction pair,
75 in which all the objects of the tribosystem are involved: the bearing, the counterbody and the
76 lubricant. In this case, the data given in Table 1, are the average values over a visible area of $0.553 \times$
77 0.553 mm. However, the process of friction at the micro level can be represented as the friction of a
78 number of separate local areas, different in mechanical and chemical properties. Thus, various
79 conditions are locally provided for the formation of secondary structures, and as a result, their
80 composition can differ significantly from one structural zone to another. Complex multicomponent
81 alloying firstly, allows increasing the strength of the aluminum matrix, making it possible to use for

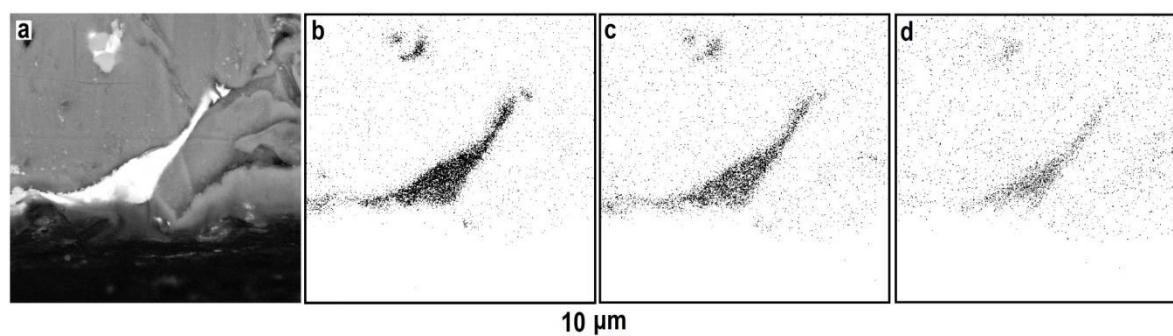
82 monometallic bearings production. Secondly, the introduction of such elements as tin and lead leads
 83 to an improvement in tribotechnical properties. Tin in the solid state in aluminum is practically
 84 insoluble and is present in the aluminum alloy in the form of soft structural constituents.



85
 86 **Figure 1.** AO-5.8 alloy surface, where: (a) SEM image of surface structure before friction; (b) SEM
 87 image of surface structure after friction; (c) tin distribution map (EDX) on the friction surface; (d)
 88 calcium distribution map (EDX).

89 The distribution maps of elements (Fig. 1c, d) on the friction surface of the alloy demonstrate
 90 that the formation of secondary structures in a number of cases is not accidental. For all samples of
 91 the experimental alloys, a match was found between the pairs of lead and sulfur elements, tin and
 92 calcium. In both cases, the alloy component reacted with the element from the lubricant, forming
 93 more stable compounds. Thus, the lubricant is able to decompose into components during operation
 94 period, some of which react with the alloy elements, the other part with the steel elements. These
 95 same processes explain six times the amount of carbon increased on the friction surface and five
 96 times that of oxygen. As a consequence, the secondary structures are metal-polymer films of
 97 different composition on the friction surface [9, 11].

98 Tin is capable of spreading over a considerable area during friction due to its ductility and
 99 fusibility, thus contributing to the mass transfer of other elements such as lead, which forms a
 100 low-melting eutectic with tin, and zinc, which increases the strength of this eutectic and its
 101 tribological properties [12, 13]. This process, in turn, increases the localization of the formation of
 102 thin lead films capable of actively interacting with fatty acids and non-metals in the composition of
 103 lubricants to form lead soaps, acting like solid lubricant.



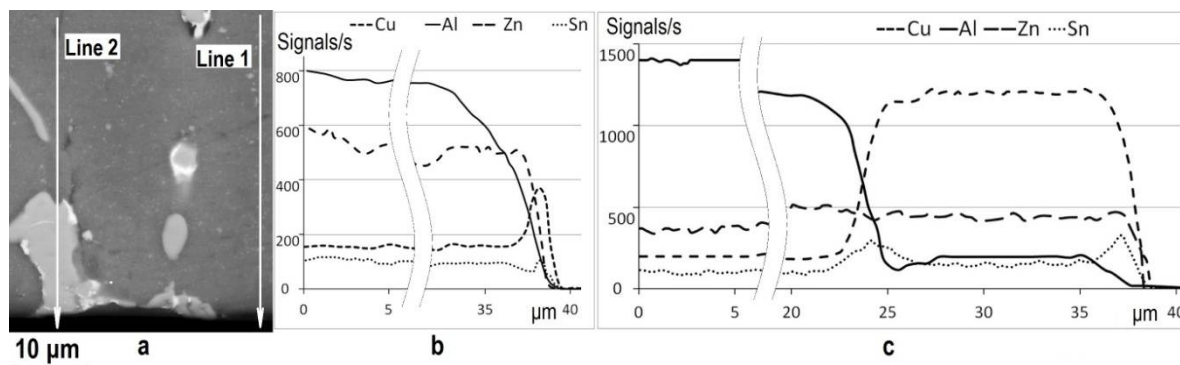
104
 105 **Figure 2.** AO-5.8 alloy subsurface layer, where: (a) SEM image of subsurface structure after friction;
 106 (b) tin distribution map (EDX) on the friction surface; (c) calcium distribution map (EDX); (d)
 107 potassium distribution map (EDX).

108 Copper, which is introduced into the alloy to increase strength, forms a solid solution with
 109 aluminum, and is also present in the alloy as solid intermetallic inclusions of CuAl_2 [14]. During the
 110 run-in process, such inclusions as well as silicon ones, wear out more slowly than the aluminum
 111 matrix, realizing the Charpy principle on the surface and forming a beneficial oil-retaining
 112 microrelief, which also contributes to the formation of secondary structures. This makes it possible
 113 to increase score resistance due to cutting of the adhesion foci with steel, but at the same time its

114 wear is increased due to a more intensive transfer of iron-containing particles to the surface. This
 115 explains the increased iron content on the friction surface of the alloy.

116 In the subsurface layer of the alloy, the changes occur to a depth of up to 100 μm . In Figure 2a
 117 area of the aluminum matrix is seen with an outlet of tin inclusion to the surface. According to the
 118 geometry of the cavity containing it, this outlet was provoked by plastic deformation of the surface
 119 layer and a physical decrease in the volume of the cavity, leaving, thus, the only possible direction
 120 for the output of the inclusion. However, it has been revealed that the components of a
 121 semidecomposed lubricant are able to form compounds not only on the friction surface, but also to
 122 penetrate through diffusion depthward to the alloy (Figure 2b, c, d). First of all, this is true for tin,
 123 calcium and potassium, as well as for a pair of lead-sulfur.

124 To determine the relative changes in the elements of the bearing material versus depth of
 125 penetration, an energy-dispersive analysis along the line was performed (Figure 3). The distribution
 126 character of curves changes depending on the local area is being analyzed (Figure 3 b, c). In the area
 127 without inclusions, aluminum, the main component of the matrix, gradually wears out during the
 128 friction process (Fig. 3b). Aluminum-depleted layer is about 5-7 micrometers. The same character of
 129 the distribution curves has the majority of alloying components, for example, zinc (Figure 3b).
 130 Although it is obvious that its content on the surface is higher relative to the matrix in which it is
 131 predominantly dissolved than in the initial state. The content of copper in the subsurface layer
 132 increases sharply. This is probably due to the difference in the wear rate of the softer aluminum
 133 matrix and copper inclusions: aluminum wears out more per time unit, increasing the proportion of
 134 copper in the total composition of the subsurface layer. A small tendency toward an increase in
 135 content, accompanied by a preliminary weak decrease, is shown by tin and, as a consequence, its
 136 satellites: calcium and potassium. Just an increase in concentration would mean that tin could be
 137 deposited from other sites by "smearing" the surface. However, the presence of a depleted region on
 138 the graph allows us to infer the forced transfer ("pumping") of this element from the subsurface layer
 139 to the friction surface.



140

141 **Figure 2.** AO-5.8 alloy elements distribution depthward: (a) elements distribution along line 1; (b)
 142 elements distribution along line 2.

143 Tin directly in the form of inclusions on the straight line being analyzed is absent, but there are
 144 areas enriched by this element at the boundary of the aluminum matrix and copper inclusion, and
 145 also in the region where this inclusion enters the friction surface. Thus, the increased content of
 146 copper-based solid sections is accompanied by a more intense formation of secondary structures
 147 containing tin on them. Solid inclusions can increase the hardness of the alloy due to its mechanical
 148 properties, while in the process of friction they also act as abrasive particles, which increase the wear
 149 of the steel counterweight and increase the coefficient of friction. Tribosystem in the process of
 150 self-organization minimizes these negative aspects of friction by forming secondary structures that
 151 include tin alloy and lubricant components: polymer base, calcium, potassium. The thickness of such
 152 a film is less than 1 μm , so that electrons from scanning microscope, reaching the formations under
 153 the secondary structures, allow recording the base signal.

154 **4. Conclusions**

155 During the run-in, the friction surface undergoes not only structural changes, but also
156 component composition changes by the formation of profitable secondary structures. In their
157 formation, to various degrees, all the objects of the tribosystem are involved, and the secondary
158 structures themselves differ in composition in different sections of the alloy. Thus, the manufactured
159 bearing is a "workpiece", the final processing of which before the output to the operating parameters
160 during the friction process is carried out at the stage of running-in with the flow of self-organization
161 processes. The variety of alloying components determines the freedom degree of the tribosystem for
162 the formation of secondary structures.

163 This section is not mandatory, but can be added to the manuscript if the discussion is unusually
164 long or complex.

165 **Funding:** This research was funded of Ministry of Education and Science of Russian Federation
166 within the Agreement on grant № 14.574.21.0179 of September 26. 2017, unique identification
167 number RFMEFI57417X0179.

168 **Author Contributions:** conceptualization, I.G. and A.M.; methodology, P.P. and A.M.; validation, P.P., A.M.
169 and E.K.; formal analysis, A.M.; investigation, P.P.; resources, E.K, P.P. and A.M; data curation, E.K.;
170 writing—original draft preparation, P.P.; writing—review and editing, I.G. and A.M.; visualization, P.P.;
171 supervision, I.G. and A.M.; project administration, I.G. and E.K.

172 **Conflicts of Interest:** The authors declare no conflict of interest.

173 **References**

- 174 1. Lu, Z. C.; Gao, Y.; Zeng, M.Q. Improving Wear performance of dual-scale Al -Sn alloys. The role of Mg
175 addition in enhancing Sn distribution and tribolayer stability. *Wear* **2014**, *309*, 216-225, DOI:
176 10.1016/j.wear.2013.11.018.
- 177 2. Stolyarova, O.O. et al. Investigation of tribological properties and structure of new aluminum bearing
178 alloys. *Materialovedenie* **2014**, № 8, 12-17 (in Russian).
- 179 3. Belov, N.; Mironov, A. et al. *Aluminum alloys for antifriction applications*, 1st ed.; MISIS: Moscow, Russia,
180 2016; 222 p., ISBN: 978-5-906848-22-8.
- 181 4. Mironov, A.E.; Gershman, I.S. et al. Aluminum casting antifriction alloys with increased capacity to
182 adaptability of friction surfaces. *Vestnik «VNIIZhT»* **2017**, *76*, 336-340, DOI:
183 10.21780/2223-9731-2017-76-6-336-340.
- 184 5. Babu, M.V.; Rama Krishna, A.; Suman, K.N.S. Review of Journal Bearing Materials and Current Trends.
185 *Am. J. Mater. Sci. Technol.* **2015**, *2*, 72-83. DOI: 10.7726/ajmst.2015.1006.
- 186 6. Fox-Rabinovich, G; Veldhuis, S.C. et al. Features of self-organization in ion modified nanocrystalline
187 plasma vapor deposited AlTiN coatings under severe tribological conditions. *J. Appl. Phys.* **2007**, *102* (7),
188 DOI: 10.1063/1.2785947.
- 189 7. Rusin, M; Skorentsev, A.L.; Kolubaev, E.A. Dry friction of pure aluminum against steel. *J Frict. Wear+* **2016**,
190 *37* (1), 109-118, DOI: 10.3103/S1068366616010141.
- 191 8. Österreicher, J.A.; Papenberg, N.K. et al. Quantitative prediction of the mechanical properties of
192 precipitation-hardened alloys with special application to Al-Mg-Si. *Mater. Sci. Eng. A.* **2017**, *703*, 380-385.
193 DOI: 10.1016/j.msea.2017.07.080
- 194 9. Lu, Z.C.; Zeng, M.Q. et al. Improving wear performance of CuSnSb alloys through forming
195 self-organized graphene/Bi nanocomposite tribolayer *Wear* **2016**, *364-365*, 122-129. DOI:
196 10.1016/j.wear.2016.07.014.
- 197 10. Gorlenko, A.O.; Davydov, S.V.; Erokhin, A.N. Tribodiagnostics spherical plain bearings. *Handbook. An*
198 *Engineering Journal* **2017**, 9-13. DOI: 10.14489/hb.2017.12.pp.009-013.
- 199 11. Piskarev, A.S.; Sil'chenko, O.B. et al. Analysis of structural solutions at design of high-loaded sliding
200 bearings with liquid lubricants. *Vestnik Mashinostroeniya* **2018**, *5*, 37-43.
- 201 12. Springer, H.; Szczepaniak, A.; Raabe, D. On the role of zinc on the formation and growth of intermetallic
202 phases during interdiffusion between steel and aluminium alloys. *Acta Mater.* **2015**, *96*, 203-211. DOI:
203 10.1016/j.actamat.2015.06.028.

- 204 13. Kiran, T.S. et al. Effect of heat treatment on tribological behavior of zinc aluminum alloy reinforced with
205 graphite and SIC particles for journal bearing. *Ind. Lubr. Tribol.* **2015**, *67*, 292-300. DOI:
206 10.1108/ilt-08-2013-0090.
- 207 14. Menshikova, S.G.; Shirinkina, I.G. et al. A study of the structure and properties of aluminum alloys with
208 copper produced under superfast cooling of melt. *Met. Sci. Heat. Treat+* **2018**, *3*, 45-52.